A phase-field investigation of recrystallization boundary migration into heterogeneous deformation energy fields: Effects of dislocation boundary sharpness

Li, R.; Yadav, V. ; Moelans, N. ; Zhang, Y.; Juul Jensen, D.

Published in:
I O P Conference Series: Materials Science and Engineering

Link to article, DOI:
10.1088/1757-899X/1121/1/012013

Publication date:
2021

Document Version
Publisher's PDF, also known as Version of record

A phase-field investigation of recrystallization boundary migration into heterogeneous deformation energy fields: Effects of dislocation boundary sharpness

R Li[1], V Yadav[2], N Moelans[2], Y Zhang[1] and D Juul Jensen[1]

[1] Department of Mechanical Engineering, Technical University of Denmark, 2800 Kgs. Lyngby, Denmark
[2] Department of Materials Engineering, KU Leuven, Kasteelpark Arenberg 44 Bus 2450, Leuven 3001, Belgium

E-mail: rulia@dtu.dk

Abstract. The migration of recrystallization boundaries into spatially varying deformation energy fields are simulated based on a two-dimensional phase-field model. The energy fields are chosen as idealized versions of deformation microstructures subdivided by two sets of intersecting geometrically necessary dislocation boundaries (GNBs), and effects of the sharpness of the GNBs are investigated. The simulations show that the shape of the recrystallizing grain as well as the recrystallization kinetics are considerably affected by the wall characteristics of the GNBs. Recrystallization occurs faster in the deformed matrix with "sharper" walls. The simulation results highlight the importance of the deformation microstructure characteristics on the recrystallization kinetics, and as the deformation microstructures depend on the initial grain orientations, the results also indicate tight relations between initial, deformation and recrystallization textures.

1. Introduction

Annealing of a deformed metal typically leads to recrystallization by which the deformed grains are replaced by new almost perfect grains: A recrystallized grain has a much lower density of dislocations than that in the deformed matrix [1]. The driving force for recrystallization is generally assumed to be the energy stored in the matrix in the form of defects and dislocations created by plastic deformation [1,2]. Only recently has it been demonstrated that curvature driving and dragging forces related to sharp retrusions and protrusions on migrating recrystallization boundaries may be of the same order of magnitude [3]. Important for both the local stored energy distribution and the curvature forces is how the dislocations are arranged in the matrix. This distribution is, in almost all cases, heterogeneous, as the dislocations arrange to minimize their energy as much as possible into low energy dislocation structures [4]. On the grain scale, the common framework is that the dislocations tend to form structures with a high dislocation density in geometrically necessary boundaries (GNBs) separating regions with much lower dislocation densities from each other. For an overview, see [5]. The driving force for recrystallization thus varies along the recrystallization boundaries, and the boundary profile may change, reflecting how the local dislocation structures are absorbed [6–8]. An important insight

from a texture perspective is that grains with different crystallographic orientations deform following this common framework but with different arrangements and types of dislocation boundaries, for example some being on {111} planes, others not [9].

The growth of recrystallized grains has been well characterized by three-dimensional X-ray microscopy in the bulk of commercially pure aluminum [8,10–12], revealing a heterogeneous growth pattern, with irregular protrusions and retrusions of different amplitudes and widths. It has been suggested that the size and shape of the protrusions and retrusions are correlated in a relatively complex way to the spatial variations in stored energy [11]. A serious complication when interpreting the experimental results is the large number of parameters affecting the recrystallization boundary migration, many of which are correlated to each other, and many of which are not known. Numerical simulations provide potent tools to investigate effects of all these parameters *individually*. As a very general technique, the phase-field method introduces order parameters to track the microstructure evolution in specific phase fields. The method has proved very suitable for modeling complex morphological processes, *e.g.*, grain growth [13], solidification [14], and precipitation [15]. As to the study of recrystallization, it is also possible to introduce specific deformation microstructures into a phase-field model. The movement of an initially planar boundary during recrystallization was simulated using a relatively simple 1D deformation field [6], and most recently, Yadav *et al.* [7] studied effects of the 2D geometrical alignment of dislocation boundaries on the recrystallization boundary migration, revealing the complexity of recrystallization in heterogeneous energy fields. In these papers, a sinusoidal function was used to represent the microstructural variations. This corresponds to relatively broad dislocation boundaries and a smoothly varying deformation field. Experimentally the GNBs are often seen as sharp, narrow boundaries, and the dislocation density variations may thus in reality be more abrupt. The aim of the present work is to study effects of this on recrystallization by stimulating the growth of an initially circular nucleus in three deformation fields with the same average stored energy but with the majority of the energy concentrated in more or less sharp boundaries.

2. Simulation details

The phase-field model employed in this paper is inspired by the simulation works of Moelans [6,16]. The primary strategy is introducing two order parameters $\eta_{\mathrm{rex}}(x,y,t)$ and $\eta_{\mathrm{def}}(x,y,t)$, which are continuous functions of the spatial coordinates and time, to distinguish different states of the system, with $\eta_{\mathrm{rex}}, \eta_{\mathrm{def}} = 1, 0$ and $\eta_{\mathrm{rex}}, \eta_{\mathrm{def}} = 0, 1$ in the recrystallizing grain, and deformed matrix, respectively. The thermodynamic free energy (F) is assumed to consist of contributions from the grain boundary energy (F_{gb}) and the stored energy (F_{def}), which can be described as

$$F_{gb} = \int M\left(\frac{\eta_{rex}^4}{4} + \frac{\eta_{def}^4}{4} - \frac{\eta_{rex}^2}{2} - \frac{\eta_{def}^2}{2} + 1.5\eta_{rex}^2\eta_{def}^2 + 0.25\right) + \frac{\kappa}{2}((\nabla\eta_{rex})^2 + (\nabla\eta_{def})^2)\,\mathrm{d}\Omega \quad (1)$$

$$F_{def} = \int f_{def}(x,y)\frac{\eta_{def}^2}{\eta_{rex}^2+\eta_{def}^2}\,\mathrm{d}\Omega \quad (2)$$

where f_{def} is the local stored energy density. Model parameters κ, and M are related to the grain boundary energy and the diffuse interface width (ℓ_{gb}).

A Fourier-spectral method with semi-implicit time-stepping was employed to update the order parameters based on the assumption of periodic boundary conditions [17]. Simulations parameters used in this paper are as follows: time-step $\Delta t = 0.01$, grid spacing $\Delta x = 1$, model parameters $L = 5$, and $M = 1$, which are chosen empirically for a good balance between accuracy and computing efficiency. More details about the model can be found in [6,7].

We here idealize typical deformation microstructures by two sets of equispaced GNBs lying at equal but opposite angles of π/12 and -π/12, respectively, to the vertical axis, which for rolled samples corresponds to the rolling direction. Three kinds of f_{def} are used for the simulations:

$$f_{def,1}(x,y) = \max\left\{A_1\left[1+\sin\left(\frac{\pi}{64}\left(y-\frac{x}{\tan(\pi/12+\pi/2)}\right)\right)\right], A_1\left[1+\sin\left(\frac{\pi}{64}\left(y-\frac{x}{\tan(-\pi/12+\pi/2)}\right)\right)\right]\right\} \quad (3)$$

$$f_{def,2}(x,y) = \max\left\{A_2\left[\sin\left(\frac{\pi}{128}\left(y - \frac{x}{\tan(\pi/12+\pi/2)}\right)\right)\right]^4, A_2\left[\sin\left(\frac{\pi}{128}\left(y - \frac{x}{\tan(-\pi/12+\pi/2)}\right)\right)\right]^4\right\} + C \quad (4)$$

$$f_{def,3}(x,y) = \max\left\{A_3\left[\sin\left(\frac{\pi}{128}\left(y - \frac{x}{\tan(\pi/12+\pi/2)}\right)\right)\right]^{10}, A_3\left[\sin\left(\frac{\pi}{128}\left(y - \frac{x}{\tan(-\pi/12+\pi/2)}\right)\right)\right]^{10}\right\} + C \quad (5)$$

where $A_1 = 0.04$, $A_2 = 0.0953$, $A_3 = 0.1325$, $C = 0.001$. Figure 1a-c show the representation of $f_{def,1}$, $f_{def,2}$ and $f_{def,3}$. Cross-sectional plots of the three stored energy fields at vertical and horizontal directions are shown in figure 1d-i, which corresponds to the red and purple traces in figure 1a-c, visualizing the wall profiles. The average stored energy density values of the employed fields are the same and equal to 0.0561 in all three cases. We assumed that the spatial variations in stored energy are constant irrespective of annealing time, meaning that recovery is not considered in the simulations.

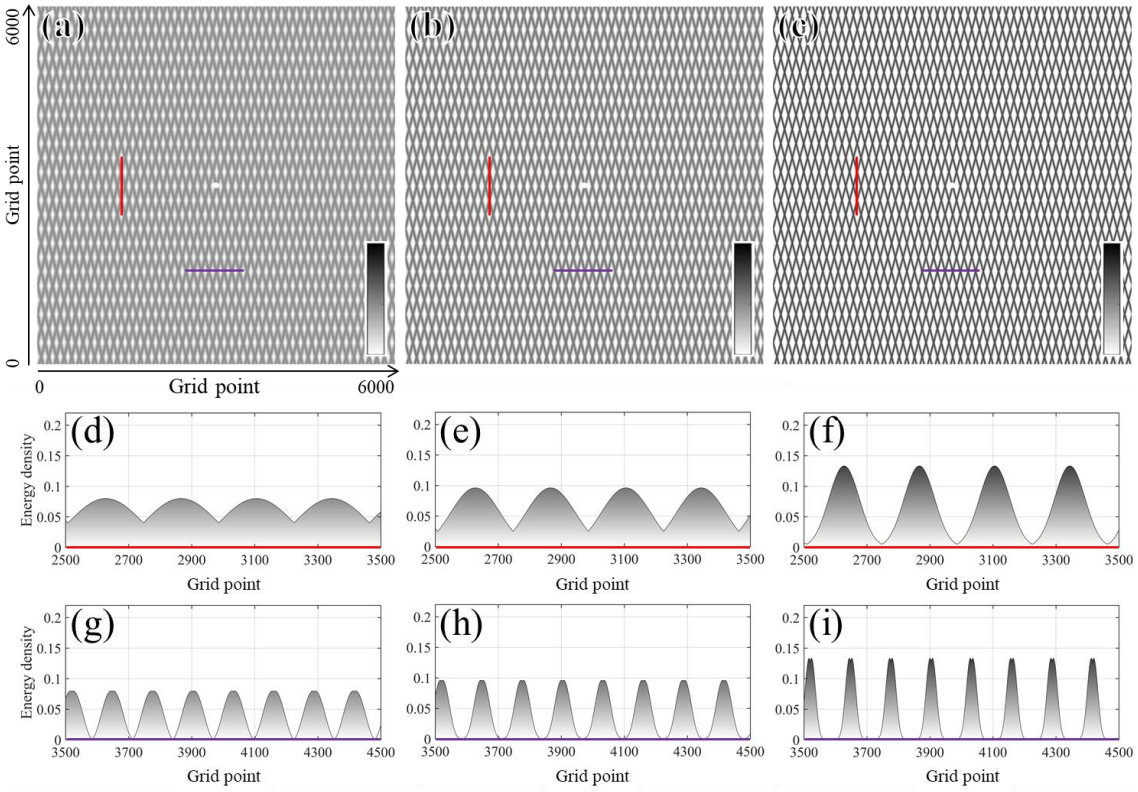

Figure 1. Representation of the employed stored energy fields and cross-sectional plots at vertical/horizontal directions. (a, d, g) $f_{def,1}$. (b, e, h) $f_{def,2}$. (c, f, i) $f_{def,3}$. The black-white scale range is here chosen to be from 0 to 0.18, with black representing the highest stored energy density. The center-positioned white circle in (a-c) represents the original nuclei (see section 3).

The system size was 6000×6000 grid points. The code was written in Julia programming language [18], which allows an efficient implementation of the Fourier-spectral method by calling a GPU (NVIDIA Quadro P5000) on an HP Z4 workstation.

3. Results and discussion

One circular nucleus/grain of radius 50 grid points were center-positioned in each of the three simulation boxes to grow (*i.e.*, recrystallize) into the different stored energy fields. Figure 2 shows the positions of the recrystallization boundary traces starting from the time-step 60000 to 260000 with an interval of 5000 time-steps. Note that only the top-right part of the simulation box is plotted, and we highlight the migration traces at the time-step of 60000, 160000, and 260000 with red lines. Figure 2a, as a reference, shows the migration traces in a uniform stored energy field, which are all perfect

circles. While as seen in figure 2b-c, the original circular boundaries migrate and change shapes while absorbing the GNBs, yielding hexagon-shaped grains in the three heterogeneous fields.

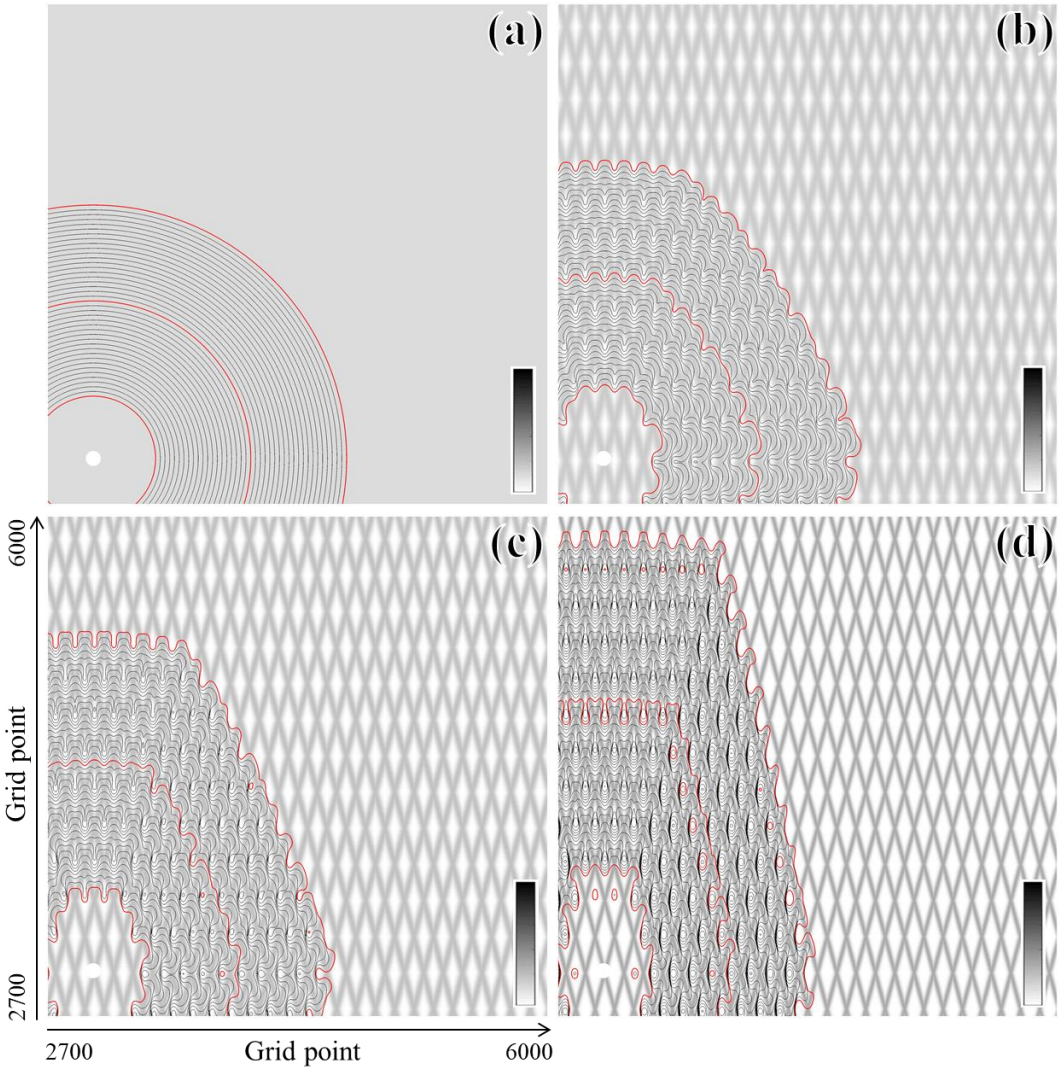

Figure 2. Recrystallization boundary traces as a function of time obtained in the simulations. (a) Uniform field. (b) $f_{def,1}$. (c) $f_{def,2}$. (d) $f_{def,3}$. The filled white circle area represents the original nuclei. The traces are plotted every 5000 time-steps starting from the time-step of 60000 to 260000. The black-white scale range is here 0 to 0.4, with black representing the highest stored energy density.

Specifically, figure 3 shows the simulated shapes of the recrystallizing grains after annealing for 260000 time-steps. It is noteworthy that while the wall-spacing, angle, and average stored energy density are the same for all the employed fields, the resultant grain shapes differ significantly, showing GNB-dependent anisotropic recrystallization behavior. Most obvious, the shape of the growing grain becomes closer to a narrow hexagon when the GNB sharpness increases as the differences in the horizontal and vertical migration rates become more apparent. The overall boundary velocities in the horizontal and vertical yield ratios of 1:1.2, 1:1.4, and 1:2.1 in $f_{def,1}$, $f_{def,2}$ and $f_{def,3}$, respectively. In all cases, the boundary positions coincide in the ~48º direction.

The migrating boundary profile is highly dynamic while moving into the heterogeneous deformation fields: protrusions transform into retrusions and vice-versa continuously, and the boundary experiences a stop-and-go type movement (boundary segments remain for a longer period at

positions with low stored energy density and then advance suddenly to the next position of similar low stored energy), which is similar to what has been observed experimentally, *e.g.*, [7]. This is more evident in the field with "sharper" walls. As the stored energy density gradient is very high in $f_{def,3}$, the curvature related driving force cannot balance the stored energy gradient. Therefore some moving boundary segments can quickly bow out, and parts of the moving boundary on both sides of the stagnated part can join thereby pinching off a part of the boundary, leaving behind isolated unrecrystallized islands of the deformed matrix. These isolated islands recrystallized upon further annealing.

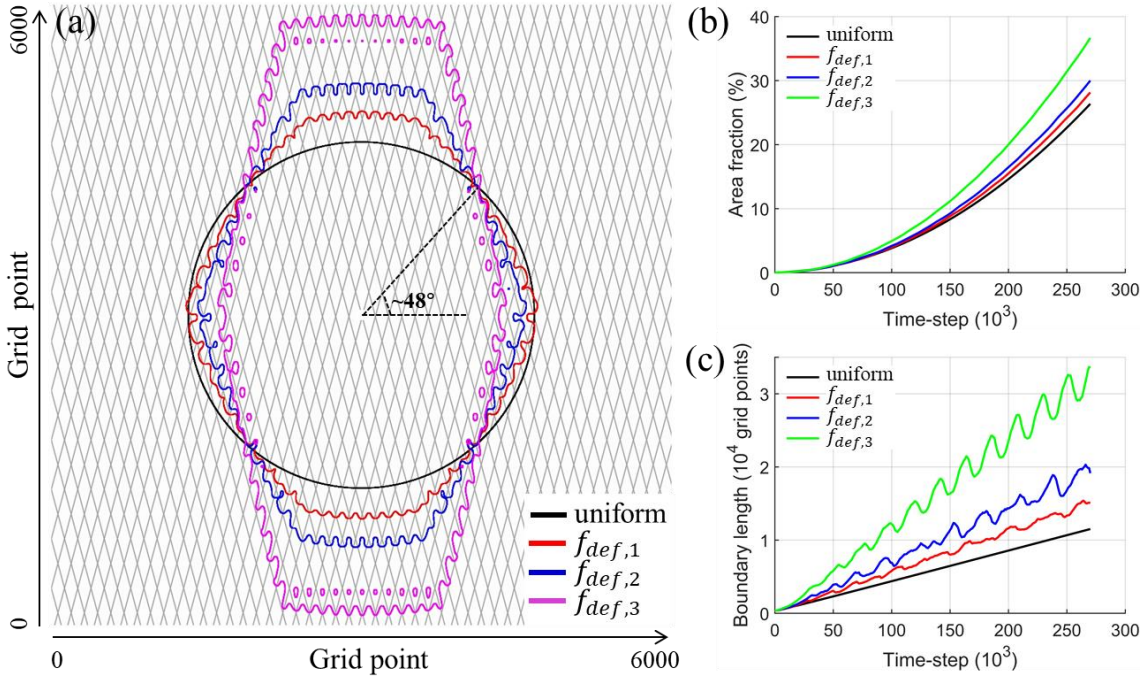

Figure 3. (a) The simulated shapes of the recrystallizing grain at the time-step of 260000 in the different stored energy fields (taken from figure 2). The simulated area fraction (b) and boundary length (c) of the recrystallizing grain in the different stored energy fields as a function of annealing time.

Figure 3b and c show the recrystallized area fraction and boundary length of the recrystallizing grain as a function of annealing time. Both values are always the largest in $f_{def,3}$ and smallest in the uniform field at any time-step, and the difference becomes more and more evident with annealing, suggesting that recrystallization occurs faster in the field with "sharper" GNBs ($f_{def,3}$). Note that the boundaries of the left behind isolated islands of deformed material are also included in both figure 3b and c. As shown in figure 3b, the increasing rate of recrystallized area fraction in $f_{def,3}$ is 40% higher than that in the uniform field after 260000 time-steps.

The simulation results also demonstrate the anomalous scenario where the recrystallization boundary length (corresponding to the grain surface area in 3D) may not always monotonously increase with annealing time but is significantly influenced by the change in boundary roughness and boundary pinch-off events, which occur when the migrating boundary meets the "sharper" GNBs (see figure 3c).

4. Conclusions

The *sharpness* of the geometrically necessary boundaries in the deformation microstructure is a dominating factor affecting the morphology of recrystallizing grains and the boundary migration velocity during annealing. Recrystallization occurs faster in deformed microstructures with "sharper"

walls. More generally, with the aid of simulations, we have demonstrated the opportunity to quantify effects of specific deformation microstructure parameters on recrystallization kinetics by introducing various microstructures into the phase-field model. Thereby effects of different parameters can be investigated *separately*, and the simulations may suggest critical experiments.

Acknowledgments
The financial support from the European Research Council (ERC) under the European Union's Horizon 2020 research and innovation programme (M4D-grant agreement No. 788567 and grant agreement No. 714754 INTERDIFFUSION ERC-2016-STG) is gratefully acknowledged.

References

[1] Humphreys F J and Hatherly M 2004 *Recrystallization and Related Annealing Phenomena* (Elsevier)
[2] Ashby M F 1980 Recrystallization and grain growth of multi-phase and particle containing materials *1st Risø international symposium on metallurgy and materials science, Risø* p 325
[3] Zhang Y, Godfrey A and Juul Jensen D 2014 In-situ investigation of local boundary migration during recrystallization *Metall Mat Trans A* **45** 2899–2905
[4] Kuhlmann-Wilsdorf D 1989 Theory of plastic deformation-properties of low energy dislocation structures *Mater Sci Eng A* **113** 1–41
[5] Hansen N and Juul Jensen D 2011 Deformed metals–structure, recrystallisation and strength *Mater Sci Technol* **27** 1229–1240
[6] Moelans N, Godfrey A, Zhang Y and Juul Jensen D 2013 Phase-field simulation study of the migration of recrystallization boundaries *Phys Rev B* **88** 054103
[7] Yadav V, Moelans N, Zhang Y and Juul Jensen D 2021 Influence of geometrical alignment of the deformation microstructure on local migration of grain boundaries during recrystallization: A phase-field study *Scripta Mater* **191** 116–119
[8] Zhang Y, Budai J, Tischler J, Liu W, Xu R, Homer E R, Godfrey A and Juul Jensen D 2017 Boundary migration in a 3D deformed microstructure inside an opaque sample *Sci Rep* **7** 1–8
[9] Huang X and Winther G 2007 Dislocation structures. Part I. Grain orientation dependence *Philos Mag* **87** 5189–5214
[10] Schmidt S, Nielsen S, Gundlach C, Margulies L, Huang X and Juul Jensen D 2004 Watching the growth of bulk grains during recrystallization of deformed metals *Science* **305** 229–232
[11] Zhang Y, Godfrey A and Juul Jensen D 2011 Local boundary migration during recrystallization in pure aluminium *Scripta Mater* **64** 331–334
[12] Juul Jensen D and Zhang Y 2020 Impact of 3D/4D methods on the understanding of recrystallization *Curr Opin Solid State Mater Sci* 100821
[13] Moelans N, Spaepen F and Wollants P 2010 Grain growth in thin films with a fibre texture studied by phase-field simulations and mean field modelling *Philos Mag* **90** 501–523
[14] Wang N, Smith N and Provatas N 2017 Investigating gas-phase defect formation in late-stage solidification using a novel phase-field crystal alloy model *Phys Rev Mater* **1** 043405
[15] Chang K and Moelans N 2015 Phase-field simulations of the interaction between a grain boundary and an evolving second-phase particle *Philos Mag Lett* **95** 202–210
[16] Moelans N, Zhang Y, Godfrey A and Juul Jensen D 2015 A phase-field simulation study of irregular grain boundary migration during recrystallization *IOP Conf Ser: Mater Sci Eng* **89** 012037
[17] Chen L Q and Shen J 1998 Applications of semi-implicit Fourier-spectral method to phase field equations *Comput Phys Commun* **108** 147–158
[18] Bezanson J, Edelman A, Karpinski S and Shah V 2017 Julia: A fresh approach to numerical computing *SIAM Rev* **59** 65–98